Nanoscale control of doped organic hole-injection layer in thermally annealed top emission organic light emitting diode

JUNWEI XU, LEI ZHANG*, HUI LIN, QUAN JIANG
Key Lab of OLED Science and Technology, Key Lab of Display Science and Technology of Sichuan Province, School of Optoelectronic Information, University of Electronic Science and Technology of China (UESTC), Chengdu 610054, People's Republic of China

Top emission organic light emitting diodes with a maximum luminance approaching 13300cd/m^2 and an improved ambient stability is fabricated by applying the thermal annealing at 200°C in vacuum after the deposition of Aluminum/Nickel-Chromium/4,4′,4″-tris[3-methylphenyl(phenyl)amino]triphenylamine: 2,3,5,6-tetrafluoro-7,7,8,8-tetracy anop -quinodimethane(Al/Ni-Cr/m-MTDATA:F4TCNQ) hole-injection stack structure. The increased luminance and relatively stable performance are attributed to the modification of doped hole-injection material morphology and changes in the metal-organic interface induced by annealing. The thermally optimized surface and nanoscale grain networks provide stronger organic contact, higher electron-hole pairs generation and higher hole mobility compared with surface and bulk morphology of unannealed hole-injection stack structure. Formation of chemical bonds across the metal-organic interface is expected as another explanation of the enhanced hole-injection efficiency.

(Received June 30, 2012; accepted November 7, 2013)

Keywords: Top emission organic light emitting diodes(TEOLEDs), Thermal annealing in vacuum, Doped hole-injection layer, Surface morphology, Metal-organic interface

1. Introduction

Top emission organic light emitting diodes (TEOLEDs) are actively developed as a novel technology for new generation of display screen as a result of TEOLED's color self-resolution, high contrast and high aspect ratio active matrix organic light emitting device(AMOLED) [1-3].

With the development of this technology, more researches are going into trying to explicate main mechanisms and processes of TEOLEDs. There is a lack of complete understanding of how hole-injection from metal anode to organic semiconductor, therefore this remains as an intriguing topic of research. In order to facilitate hole-injection from electrodes to the active organic material, the large energey mismatch between the low work function of metal anode (Al, [4] Ag, [5] Au [6]) and the energy level of hole-transport organic material must be minimized. An additional hole-injection layer is required, typtically composed of metal oxides as such as WO_3,[7] V_2O_5,[8] MoO_3,[9] and organic-based p-type materials such as poly(3,4- ethylenedioxy thiophene)-poly(4-styrenesulfonate)(PEDOT:PSS),[10]4, 4′,4″-tris[3-methylphenyl(phenyl)amino] triphenylamine: 2,3,5,6-tetrafluoro-7,7,8,8-tetracyanop-quinodimethane (m-MTDATA:F4TCNQ) [11]. Therefore, recent researches on hole-injection focus on the morphological, structural and chemical factors of the hole-injection layer inserted between anode and hole-transport layer [12].

Generally, metal anode with high reflectivity in TEOLEDs is fabricated on glass using the sputtering method because of the method's efficient thin film deposition and excellent film robustness. Despite numerous advantages of the sputtering method, it is found that defects can exist the surface of thin films when deposited by the traditional sputtering method. This would lead to negative effects on injecting hole into the organic material. Considering that the hole-injection layer is the first organic active layer adjacent to the anode, therefore the surface and bulk morphology of hole-injection layer and the interface between anode and hole-injection layer is critical in the device fabrication procedure.

Thermal annealing in vacuum is an approach to modify the properties of organic semiconductor thin film and alloys [13]. As the surface roughness of organic material become smoother, [14] different sizes and growth directions of the crystals can be generated in the organic thin film throughout the annealing treatment [15]. Meanwhile, the chemical interaction of metal-organic

interface through the heat treatment can produce chemical composite that can highly affect interface electrical property.

Herein, via thermal annealing in vacuum to fabricate Al/Ni-Cr/m-MTDATA:F4TCNQ as anode/HIL for TEOLEDs, the morphological, structural and chemical properties of m-MTDATA:F4TCNQ as the hole-injection layer abut the Ni-Cr alloy film are investigated. Furthermore, we report the luminance and efficiency characteristics of TEOLEDs with thermal annealing treated hole-injection stack at a low temperature. We have found that the annealed TEOLEDs not only display remarkably increased luminance, but is also capable of stabilizing optoelectronic properties of the fabricated device.

2. Experimental

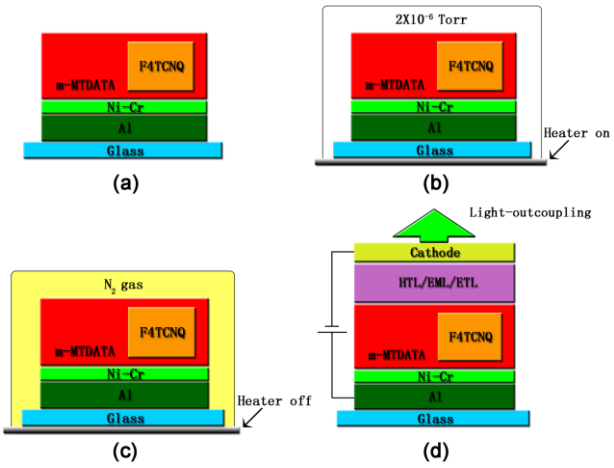

Fig. 1. The fabrication procedure of thermally annealed TEOLED: (a) hole-injection stack structure deposition; (b) thermal annealing in vacuum; (c) after cool down; (d) completed device.

In our experiments, m-MTDATA:F4TCNQ and Al/Ni-Cr were used as hole-injection layer(HIL) and anode, respectively. To fabricate high-quality hole-injection stack (Al/Ni-Cr/m-MTDATA:F4TCNQ) on contaminated glass, the glass substrates (2 cm × 2 cm) were sequentially sonicated in acetone, alkali and deionized water. The substrates were treated by O^2-plasma-treated before use. Al(80nm)/Ni-Cr(20nm) the bilayer structure of the anode, was grown by DC magnetron sputtering deposition under a vacuum of 3×10^{-6}Torr. The fabrication of hole-injection structure was then completed after a 100nm m-MTDATA doped F4TCNQ (4 vol %) was deposited by conventional thermal evaporation method at a rate of 1Å/s. The substrates holding Al/Ni-Cr/m-MTDATA:F4TCNQ were loaded into a vacuum chamber with a base vacuum of 2×10^{-6}Torr prior to turning the heater on. The temperature of hot plate was set to 200℃. Thermal annealing in vacuum lasted for 30min on the hot plate then the system was cooled down to room temperature using high-purity nitrogen gas. Fig. 1(a), 1(b) and 1(c) show the thermal annealing 3-steps procedure of hole-injection stack. Atomic force microscope (AFM; MFP-3D-Bio, Asylum Research) images were obtained to evaluate the morphologies of annealed m-MTDATA:F4TCNQ film on Al. The sheet resistivity was determined by four-point probe measurements.

The TEOLEDs with a structure of Al/Ni-Cr/m-MTDATA:F4TCNQ/NPB/Alq3:C545T/Alq 3/LiF/Al/ITO was fabricated with (NPB=N,N-bis(1-naphthyl) N,N-diphenyl-1,1-biphenyl-4,4-diamine, Alq3=tris (8-hydroxyquinoline) aluminum, ITO=indium tin oxide, and C545T=Coumarin 545 tetramethyl as the green fluorescent dye). NPB(20nm), Alq3:C545T(30nm) and Alq3(20nm) were deposited as the hole-transport layer(HTL), the emission layer(EML) and the electron-transport layer(ETL), respectively. All TEOLEDs fabricated in this paper were fabricated on glass substrates (20cm × 20cm). The fabrication of hole-injection stack structure and annealing process has been described above. Lastly the device went through thermal evaporation of HTL, EML, ETL and cathode in a chamber with a base vacuum of 2×10^{-7} Torr, as seen in Fig. 1(d). The area of the active device was 9 mm^2. Here, we used PhotoResearch 650 and Keithley 2400 to measure the electronic and luminous properties of TEOLEDs and to draw the luminance-voltage-current density and efficiency-voltage curves of the completed devices without encapsulation in the clean room at an ambient temperature of 25℃.

3. Results and discussion

Fig. 2(a), 2(b) and 2(c) show AFM images (5μm×5μm) of Al/Ni-Cr/m-MTDATA:F4TCNQ, 150℃ -annealed Al/Ni-Cr/m-MTDATA:F4TCNQ and 200℃ -annealed Al/Ni-Cr/m-MTDATA:F4TCNQ, respectively. From 3-Dimensional AFM images, the unannealed 100nm-thick m-MTDATA:F4TCNQ film covering the Ni-Cr alloy film exhibits significant spikes, conversely, the annealed surface morphology becomes smoother with the increasing annealing temperature. By comparing the corresponding 2-Dimensional AFM images of the surface of 200 ℃ -annealed Al/Ni-Cr/m-MTDATA: F4TCNQ and one without annealing, more white dots (spikes in 3-Dimensional AFM image) are observed on the latter. The quality of the first few organic layers is critical because all important charge transport process are confined to the first several monolayers.[15] The flat interfaces exhibit fewer defects and generally yield higher charge carrier mobility [17,18].

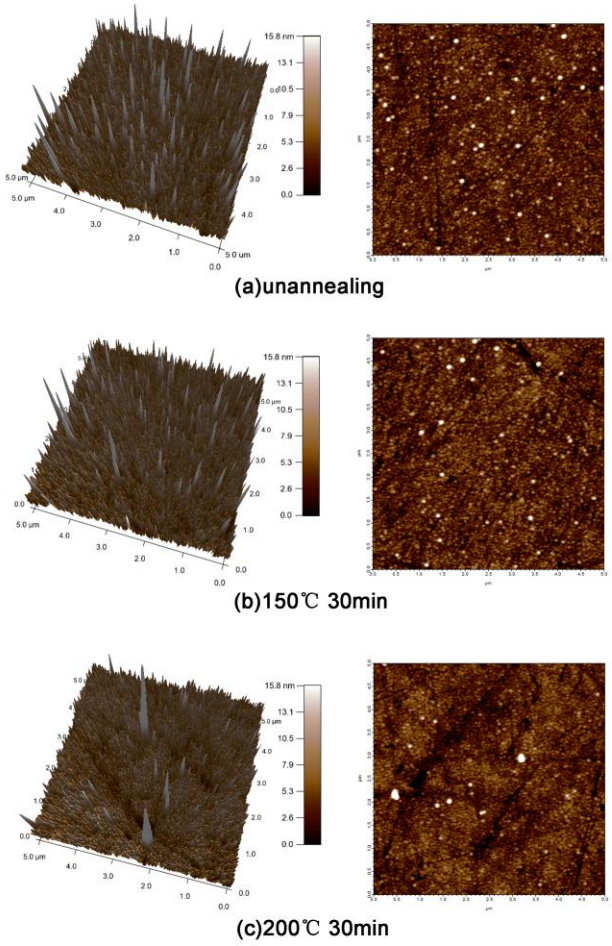

Fig. 2. Three-dimentional and two-dimentional AFM images(5um×5um) of Al/Cr-Ni/m-MTDATA:F4TCNQ stack surface morphology: (a) before thermal vacuum annealing; (b) after thermal vacuum annealing at 150 ℃ for 30 minutes; (c) after thermal vacuum annealing at 200 ℃ for 30 minutes.

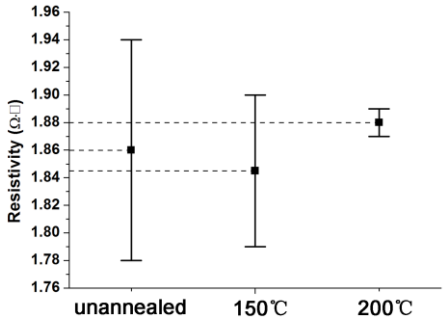

Fig. 3. Sheet resistivity of m-MTDATA:F4TCNQ films without and with thermal annealing (150 ℃ and 200 ℃).

Sufficient smoothness at the interface between hole-injection layer and hole-transport layer promotes hole-injection as a result of strong adhesion and enhanced contact area of the connective organic active layers [19]. Therefore, it is thought that the surface of annealed m-MTDATA:F4TCNQ film with less spikes form a smoother organic contact next to NPB, resulting in an efficient hole-injection at the interface. Fig. 3 presents the sheet resistivity of m-MTDATA:F4TCNQ films before and after annealing. The values of sheet resistivity are collected from various locations with different orientations. Comparing with the sheet resistivity of m-MTDATA:F4TCNQ films before heat treatment, the 200℃-annealed m-MTDATA:F4TCNQ film shows steady sheet resistivity at 1.88 Ω·□. This demonstrates that the smooth organic surface morphology appears after the annealing procedure.

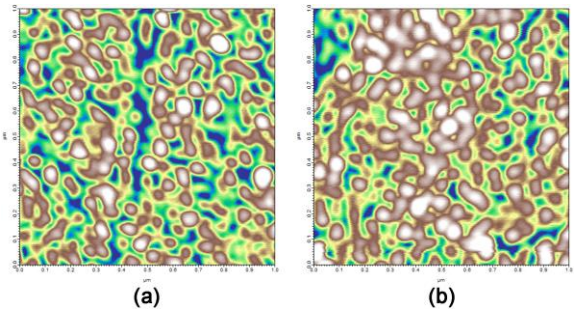

Fig. 4. AFM images(1umX1um) of m-MTDATA: F4TCNQ films: (a) islands morphology before thermal annealing; (b) the nanoscale gain networks after thermal annealing.

AFM images (1μm×1μm) of m-MTDATA: F4TCNQ grains before and after thermal annealing in vacuum are shown in Fig. 4. Without heat treatment, the m-MTDATA:F4TCNQ grains are still separated, forming small islands. The nanoscale grain networks are not well developed. After 200℃ heat treatment for 30 min, the morphology of the nanoscale grain networks becomes clearer, and crystal structure of the m-MTDATA:F4TCNQ gains has improved. It is known that the F4TCNQ serves as an acceptor in the m-MTDATA, which means that the highest occupied molecular orbital (HOMO) level of m-MTDATA is very close to the lowest occupied molecular orbital (LUMO) level of F4TCNQ. When F4TCNQ is doped in m-MTDATA, there is a high chance that F4TCNQ:m-MTDATA+ will be formed. This material is also shown to be capable of generating a large number of bounded electron-hole pairs. The formation of the interpenetrating gain networks facilitates the electron-hole pairs density and the hole mobility throughout the networks. This induces an efficient charge transfer and the formation of exciton.

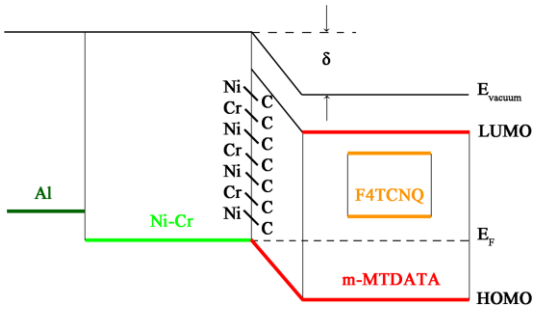

Fig. 5. Schematic diagram for the interfacial dipoles and band bending.

Recent studies have reported that chemical bonds can be formed at the metal-organic interface [20,21]. Thermal annealing on hole-injection structure might also be expected to influence the interface between m-MTDATA:F4TCNQ layer and Al/Ni-Cr electrode. As a result Ni and Cr atoms becomes heated causing metal atoms to gain enough energy to diffuse through interface. Therefore a chemical reaction exists between the m-MTDATA molecule and diffused metal atoms. The formation of chemical bonds (e.g. Ni-C or Cr-C) could leads to a layer of dipoles at the Ni-Cr/m-MTDATA: F4TCNQ interface. The dipoles across the surface would enhance the electrostatic potential energy at the interface, resulting in band bending [22]. Instead of a flat band, a bending band is formed with a narrow space charge region, where the HOMO of m-MTDATA:F4TCNQ shifts slightly upward. This indicates a strong hole-transfer from the Ni-Cr alloy atoms to the doped hole-injection m-MTDATA:F4TCNQ layer. The diagram of dipoles and bending band is shown in Fig. 5. Comparing with the hole-injection barrier with a magnitude of 0.3eV, the upwards HOMO level shift at the Ni-Cr/m-MTDATA:F4TCNQ interface reduces and even eliminates injection barrier at the anode-HIL interface. This increases the hole-injection efficiency significantly.

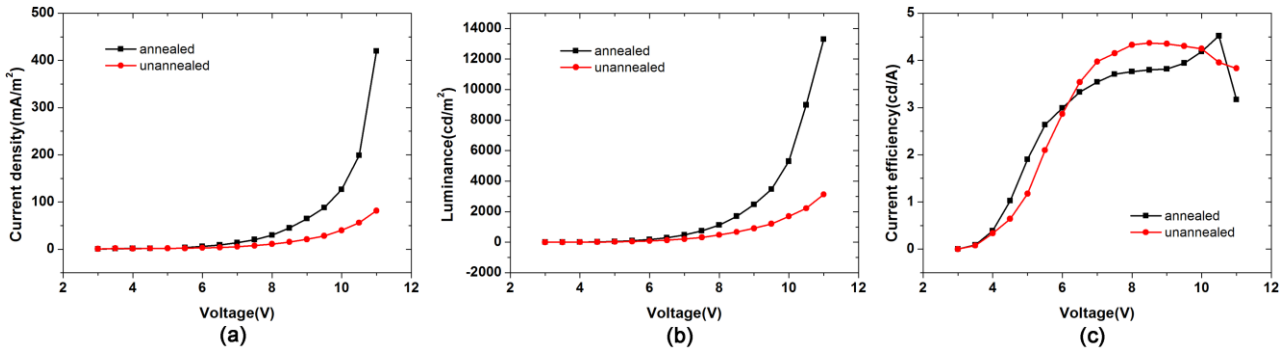

Fig. 6. Eletrical and optical characteristics of TEOLEDs with Al/Cr-Ni/m-MTDATA:F4TCNQ stack structure before and after thermally annealed : (a)I-V curves of the devices;(b)L-V curves of the devices;(c)η-V curves of the devices.

To investigate the effect of thermal annealing on the doped hole-injection layer, typical top-emitting devices were fabricated. Fig. 6 (a) and 6 (b) show the current density and luminance versus the applied voltage (I-V and L-V) before and after thermal annealing, respectively. After Al/Ni-Cr/m-MTDATA:F4TCNQ heat treatment at 200℃ for 30 min, current density increases to 420 mA/cm^2 at 11V compared with 82 mA/cm^2 of an unannealed device at the same bias, indicating that device charge transfer is improved. The device without heat treatment displays poor performance with a maximum luminance (L_{max}) of 3130cd/m^2 at the bias voltage of 11V. In contrast, the L_{max} of the annealed device can be as high as 13300cd/m^2. Fig. 6(c) exhibits the current efficiency (η) as a function of the forward bias voltage for the annealed and unannealed devices. The highest current efficiency (4.52cd/A) of annealed device reaches a luminance of 8990cd/m2, however the highest luminance of unannealed device's current efficiency (4.37cd/A) reaches only 670cd/m^2. This shows an efficient hole-injection of m-MTDATA:F4TCNQ after annealing.

The annealed and unannealed TEOLEDs without encapsulation were characterized again at ambient temperature and pressure two hours later. L-V curves are plotted in Fig. 7. Both of the devices exhibit a dramatic attenuation in the light coupling as a result of vapor infiltration and organic material oxidization. After 200℃ heat treatment, the luminance of annealed device drops to 1180 cd/m^2 at 12V, meanwhile for the unannealed device a weak light emission of 6.99 cd/m^2 at a low applied voltage is outputted and then breaks down in a few seconds. Additionally, it is surprising that the annealed device shows an increase in current efficiency (6.89 cd/A). This implies that thermal annealing for hole-injection layer on metal anode is a promising method to fabricate superior and stable TEOLEDs.

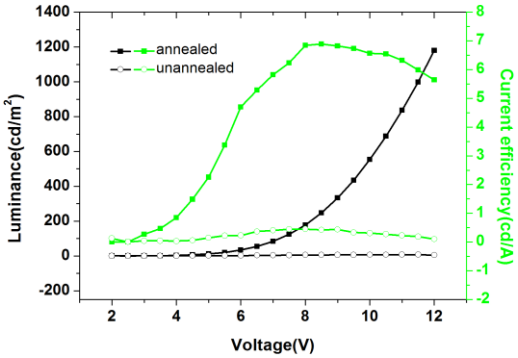

Fig. 7. L-V-ηcharacteristics of TEOLEDs with thermal annealed Al/Cr - Ni/m - MTDATA : F4TCNQ stack structure 2 hours later.

4. Conclusions

Based on the result above, we find out thermal annealing on in vacuum is an efficient method to improve TEOLEDs' luminance and stability. The luminance of annealed device increases by 10.9% compared with that of unannealed device at same current density (82mA/m^2). We attribute the improved performance and stability to changes in the surface and bulk morphology of doped hole-injection material and anode-HIL interface. The reformation of m-MTDATA: F4TCNQ film surface morphology reduces spikes significantly leading to the conclusion for an enhanced contact adhesion and strength with NPB. Under heat treatment, separated m-MTDATA grains recrystallize and combine to form nanoscale networks that promote electron-hole pairs generation and hole carrier mobility. Meanwhile, band bending upward induced by dipoles at metal-organic interface lowers the hole barrier blocking charge transfer from metal anode, resulting in an increased hole-injection efficiency from anode to HIL.

Acknowledgment

The work was supported by Fundamental Research Funds for the Central University (Grant No. ZYGX2010J058).

References

[1] R. Cheng, C. N. Borca, N. Pilet, B. Xu, L. Yuan, B. Doudin, S. H.Liou, P. A. Dowben, Appl. Phys. Lett. **81**, 2109 (2002).
[2] Y. Li, L. W. Tan, X. T. Hao, K. S. Ong, F. Zhu, L. S. Hung, Appl. Phys. Lett. **86**, 153508 (2005).
[3] T. Sekitani, H. Nakajima, H. Maeda, T. Fukushima, T. Aida, K. Hata, T. Someya, Nat. Mater. **8**, 494 (2009).
[4] J. Y. Lee, Appl. Phys. Lett. **88**, 073512 (2006).
[5] H. W. Oh, J. W. Huh, B. Ju, C. W. Lee, Thin Solid Films **519**, 6872 (2011).
[6] H. M. Zhang, W. C. H. Choy, J. Phys. D: Appl. Phys. **41**, 062003(2008).
[7] C. C. Chang, S. W. Hwang, C. H. Chen, J. F. Chen, Jpn. J. Appl. Phys. Part1 **43**, 6418 (2004).
[8] T. Matsumoto, T. Nakada, J. Endo, K. Mori, N. Kavamura, A. Yokoi, J. Kido, SID Int. Symp. Digest Tech. Papers **4**, 979 (2003).
[9] C. W. Chen, Y. J. Lu, C. C. Wu, E. H. E. Wu, C. W. Chu, Y. Yang, Appl. Phys. Lett. **87**, 241121 (2005).
[10] T. A. Heameed Shahul, M. R. Baiju, J. Aneesh, P. Predeep, Optoelectron. Adv. Mater. -Rapid Comm. **6**, 91(2012).
[11] M. K. Fung, K. M. Lau, S. L. Lai, C. W. Law, M. Y. Chan, C. S. Lee, S. T. Lee, J. Appl. Phys. **104**, 034509 (2008)
[12] J. C. Scott, J. Vac. Sci. Technol. **21**, 521 (2003)
[13] H. S. Liu, W. M. Yang, C. C. Dun, Y. C. Zhao, L. M. Dou, Optoelectron. Adv. Mater. -Rapid Comm. **6**, 95(2012).
[14] S. Sepeai, M. M. Salleh, M. Yahaya, A. A. Umar, Thin Solid Films **517**, 4679 (2009).
[15] D. H. Zhang, D. E. Brodie, Thin Solid Films **238**, 95 (1994).
[16] G. Hlawacek, P. Puschnig, P. Frank, A. Winkler, C. Ambrosch- Draxl, C. Teichert, Science **321**, 108 (2008).
[17] S. Steudel, S. D. Vusser, S. D. Jonge, D. Janssen, S. Verlaak, J. Genoe, P. Heremans, Appl. Phys. Lett. **85**, 4400 (2004).
[18] H. Yan, S. Swaraj, C. Wang, I. Hwang, N. C. Greenham, C. Groves, H. Ade, C. R. McNeill, Adv. Funct. Mater **20**, 4329 (2010).
[19] G. W. Choi, Y. J. Seo, K. Y. Lee, W. S. Lee, J. Vac. Sci. Technol. A **25**, 999 (2007).
[20] J. X. Tang, C. S. Lee, T. Lee, Appl. Surf. Sci. **252**, 3948 (2006).
[21] Y. Hirose, A. Kahn, V. Aristov, Phys. Rev. B **54**, 13748 (1996).
[22] M. G. Helander, Z. B. Wang, J. Qiu, M. T. Greiner, D. P. Puzzo, Z. W. Liu, Z. H. Lu, Science **332**, 944 (2011).

*Corresponding author: zlei@uestc.edu.cn